Precision Medicine and Imaging

Clinical Cancer Research

TERT Promoter Mutation Detection in Cell-Free Tumor-Derived DNA in Patients with *IDH* Wild-Type Glioblastomas: A Pilot Prospective Study

Tareq A. Juratli[1], Sebastian Stasik[2], Amir Zolal[1], Caroline Schuster[3], Sven Richter[1], Dirk Daubner[4], Mazen A. Juratli[5], Rachel Thowe[6], Silke Hennig[1], Meriem Makina[1], Matthias Meinhardt[7], Tim Lautenschlaeger[6], Gabriele Schackert[1,8], Dietmar Krex[1,8], and Christian Thiede[2]

Abstract

Purpose: We conducted a pilot study to assess the feasibility and the potential implications of detecting *TERT* promoter (*TERT*p)–mutant cell-free tumor-derived DNA (tDNA) in the cerebrospinal fluid (CSF) and plasma of glioblastoma patients.

Experimental Design: Matched CSF and plasma samples were collected in 60 patients with glial tumors. The CSF collection was obtained during surgery, before any surgical manipulation of the tumor. The extracted tDNA and corresponding tumor DNA samples were analyzed for *TERT*p and isocitrate dehydrogenase (*IDH)* hotspot mutations. In addition, the variant allele frequency (VAF) of *TERT*p mutation in the CSF-tDNA was correlated with tumor features and patients' outcome.

Results: Thirty-eight patients had *TERT*p-mutant/*IDH* wild-type glioblastomas. The matched *TERT*p mutation in the CSF-tDNA was successfully detected with 100% specificity (95% CI, 87.6–100%) and 92.1% sensitivity (95% CI, 78.6–98.3%) ($n = 35/38$). In contrast, the sensitivity in the plasma-tDNA was far lower [$n = 3/38$, 7.9% (95% CI, 1.6–21.4%)]. We concordantly observed a longer overall survival of patients with low VAF in the CSF-tDNA when compared with patients with high VAF, irrespective of using the lower quartile VAF [11.45%; 14.0 mo. (95% confidence interval, CI, 10.3–17.6) vs. 8.6 mo. (95% CI, 4.1–13.2), $P = 0.035$], the lower third VAF [13%; 15.4 mo. (95% CI, 11.6–19.2) vs. 8.3 mo. (95% CI, 2.3–14.4), $P = 0.008$], or the median VAF [20.3%; 14.0 mo. (95% CI, 9.2–18.7) vs. 8.6 mo. (95% CI, 7.5–9.8), $P = 0.062$] to dichotomize the patients.

Conclusions: This pilot study highlights the value of CSF-tDNA for an accurate and reliable detection of *TERT*p mutations. Furthermore, our findings suggest that high *TERT*p mutation VAF levels in the CSF-tDNA may represent a suitable predictor of poor survival in glioblastoma patients. Further studies are needed to complement the findings of our exploratory analysis. *Clin Cancer Res; 24(21); 5282–91. ©2018 AACR.*

Introduction

Our knowledge about molecular markers in gliomas has undergone a rapid evolution in the last few years. Subsequently, a new generation of biomarkers has become available with the discovery of the genetic alterations that are responsible for the initiation and progression of gliomas, including telomerase reverse transcriptase promoter (*TERT*p) and isocitrate dehydrogenase (*IDH*) mutations (1–5).

*TERT*p mutations are one of the most common recurrent alterations (90%) in glioblastomas and were found to be clonal in both pretreatment and posttreatment autopsy samples in most glioblastoma patients (6). Moreover, the presence of somatic *TERT*p mutations in glioblastomas confers a dismal prognosis (7, 8). In contrast, only a minority of glioblastomas harbor *IDH1* mutations (5%) and were shown to represent a distinct subset with favorable outcomes (5, 8). Consequently, screening for

[1]Department of Neurosurgery, Universitätsklinikum Carl Gustav Carus, Technische Universität Dresden, Dresden, Germany. [2]Department of Medicine I, Universitätsklinikum Carl Gustav Carus, Technische Universität Dresden, Dresden, Germany. [3]AgenDix GmbH, Dresden, Germany. [4]Institute of Neuroradiology, Universitätsklinikum Carl Gustav Carus, Technische Universität Dresden, Dresden, Germany. [5]Department of General and Visceral Surgery, University Hospital Frankfurt, Goethe-University, Frankfurt am Main, Germany. [6]Department of Radiation Oncology, Indiana University School of Medicine, Indianapolis, Indiana. [7]Neuropathology, Institute of Pathology, Universitätsklinikum Carl Gustav Carus, Technische Universität Dresden, Dresden, Germany. [8]German Cancer Consortium (DKTK) Dresden and German Cancer Research Center (DKFZ), Heidelberg, Germany.

Note: Supplementary data for this article are available at Clinical Cancer Research Online (http://clincancerres.aacrjournals.org/).

T.A. Juratli and S. Stasik contributed equally to this article.

D. Krex and C. Thiede contributed equally to this article.

Corresponding Authors: Tareq A. Juratli, University Hospital Carl Gustav Carus, TU Dresden, 01307 Dresden, Germany. Phone: 0049-351-4584909; E-mail: Tareq.Juratli@uniklinikum-dresden.de; and Christian Thiede, Department of Medicine I, Universitätsklinikum Carl Gustav Carus, Fetscherstr. 74, 01307 Dresden, Germany. E-mail: Christian.Thiede@uniklinikum-dresden.de

doi: 10.1158/1078-0432.CCR-17-3717

Translational Relevance

A clinical need exists to develop sensitive and specific biomarkers for glioblastoma diagnosis and recurrence detection. Recent studies have reported highly recurrent mutations in the *TERT* promoter (*TERT*p) region in >90% of glioblastomas. These mutations have been further shown to be clonal and to confer a dismal prognosis. Consequently, if *TERT*p mutations could be detected in the cerebrospinal fluid (CSF) or plasma, this alteration could serve as a sensitive biomarker for glioblastomas. In this pilot study, we have established a clinical assay to detect *TERT*p mutations in the CSF-tDNA in patients with *TERT*p-mutant/*IDH* wild-type glioblastomas with 100% specificity and 92.1% sensitivity. In addition, we show an independent association between the *TERT*p mutation variant allele frequency in the CSF-tDNA and patients' survival. Although of exploratory nature, our results suggest that *TERT*p mutation detection in the CSF-tDNA has the potential to be a sensitive diagnostic tool in the management of glioblastoma patients.

*TERT*p and *IDH1* mutations in glioblastoma patients is of clinical value in survival prediction.

The tDNA contains identical genetic alterations to those detected in the primary tumor itself. Therefore, in numerous cancer types, circulating tDNA detection in the plasma has been shown to be a reliable tool for monitoring, diagnosis, and prognostication (9–15). However, in primary and metastatic brain tumors, the levels of tDNA in the plasma are low and inconsistently detectable (12). Moreover, tDNA assessment has not yet been established in the clinical management of glioma patients and, to date, no study has systematically evaluated the clinical value of *TERT*p mutation detection in the plasma or cerebrospinal fluid (CSF) in a large cohort of *IDH* wild-type glioblastomas.

With this in mind, we conducted a pilot prospective study to assess *TERT*p and *IDH* hotspot mutations in the CSF-tDNA and plasma-tDNA, collected during surgery. We exclusively evaluated data from patients with *TERT*p-mutant/*IDH* wild-type glioblastomas to reduce potential confounders. A further intention of our study is to explore a putative association between the burden of the *TERT*p mutation in the tDNA and patients' outcome.

Materials and Methods

Study population and intraoperative sample collection

Specimens were collected between July 2015 and September 2017 at the time of surgery from 60 patients who underwent tumor resection of newly diagnosed intracranial tumors that were suspicious for a diffuse glioma. Upon general anesthesia, 8 to 10 mL whole blood was withdrawn from every patient, and 2 to 4 mL CSF was collected during surgery from the tumor site. The CSF collection was performed directly after opening the dura (durotomy), before any surgical manipulation of the tumor, predominantly through dissection of the convexity subarachnoid space.

Blood and CSF samples were collected in specific tubes preserving the tDNA (cell-free DNA-BCT Tubes, Streck). For separation of plasma, blood samples were centrifuged at 300 g for 20 minutes. Without disturbing the buffy coat, the plasma layer (supernatant) was carefully removed and transferred into a new 2 mL low-bind tube. We also collected the pelleted material to assess *TERT*p mutations in the cellular fraction of the CSF. To completely remove residual cells, both plasma and CSF samples were subsequently centrifuged at 5,000 g for 10 minutes and stored at −20°C until downstream processing.

The present study was conducted according to the guidelines of the Declaration of Helsinki and has been approved by the local Ethics Committee of the Medical Faculty Carl Gustav Carus Dresden. All samples (CSF, blood, and tumor tissue) were collected with written consent from the patients.

Tumor tissue preparation and DNA extraction

Tumor tissues were taken intraoperatively and were snap frozen at −80°C. Frozen tumor tissue was sectioned using a cryotome (Cryostat Jung CM 1800; Leica). To assure a tumor cell content of at least 80% for nucleic acid extraction, control slides stained with hematoxylin and eosin were examined by the local neuropathologist (M. Meinhardt). For DNA isolation, the QIAmp DNA Mini Kit (Qiagen) was used.

Extraction and quantification of cell-free DNA

Cell-free DNA was extracted using the *Quick*-ctDNA Serum & Plasma Kit (Zymo Research) according to the manufacturer's protocols. Briefly, stored CSF and plasma samples were thawed at room temperature. Samples were incubated with proteinase K in digestion buffer for 30 minutes at 55°C in a water bath. After mixing with DNA binding buffer, samples were loaded into the Zymo-Spin III-S column assembly and centrifuged at 1,000 g for 2 minutes. After washing and centrifugation (10,000 g; 30 seconds), ctDNA was eluted in 35 µL TE-buffer (10 mmol/L Tris, 0.1 mmol/L EDTA, pH 8). The DNA concentration was measured by quantitative real-time PCR on an ABI7500 Real-Time PCR System (Applied Biosystems) using primers and probes for the ß-globin locus.

PCR amplification of the *TERT*p region

A nested PCR procedure was used to amplify the proximal *TERT* promoter covering nucleotide numbers C228T and C250T (chr5:1295228 C>T and 1295250 C>T; hg19) from plasma-tDNA samples as well as genomic cellular DNA from the tumor specimens. Primer sequences for the first PCR were 5′-GGCCGATTCGACCTCTCT-3′ (*TERT*-p-f) and 5′-AGCACCTCGCGGTAGTGG-3′ (*TERT*-p-r), amplifying a 489 bp fragment of the *TERT* promoter region. PCR was carried out using the Qiagen Multiplex PCR Kit (Qiagen) in a 50-µL solution, consisting of a Multiplex PCR Mix (1x), Q-solution (1x), 0.2 µmol/L each *TERT*-p-f/r, and 5 ng of template DNA. PCR was performed on a GeneAmp PCR System 9700 (Applied Biosystems) with an initial denaturation step at 95°C for 15 minutes, followed by 25 cycles of denaturation at 94°C for 1 minute, annealing/extension at 59°C for 3 minutes, and a final extension at 60°C for 10 minutes.

Second-round (nested) PCR was accomplished using the Q5 High-Fidelity Master Mix (New England Biolabs) and fusion-primers 5′-AGTGGATTCGCGGGCACAGA-3′ (forward) and 5′-CAGCGCTGCCTGAAACTC-3′ (reverse) to attach the Ion A and truncated P1 (trP1) adapter sequences to the amplicons, resulting in a 303 bp PCR product. Final reaction mixture (50 µL) consisted of Q5 Buffer (1x), 1 u Q5 polymerases, 0.5 µmol/L of

each fusion primer, 0.2 mmol/L dNTPs, and 1 μL of first-round PCR product as template. The PCR consisted of 30 seconds at 98°C; and 30 cycles of 5 seconds at 98°C, 10 seconds at 68°C, and 20 seconds at 72°C with a final extension at 72°C for 2 minutes.

Library preparation, sequencing, and data analysis

The PCR reactions were purified using a tworound purification process with Agencourt AMPure XP Reagent (Beckman Coulter) and eluted in 30 to 50 μL ddH_2O. The barcoded PCR products were quantified with a Qubit 2.0 fluorometer (Life Technologies) using the Qubit dsDNA HS Assay (Life Technologies) and sequenced unidirectionally on an Ion Torrent PGM NGS system (Life Technologies), according to the manufacturer's protocols (16).

Briefly, the pooled library was clonally amplified on Ion Sphere Particles (ISP) in an emulsion PCR using the Ion PGM Hi-Q OT2 Kit (Life Technologies). Enrichment of positive Ion Spheres (ISPs) was achieved using DynaBeadsMyOne streptavidin C1 beads (Life Technologies). Quantification of recovered particles was performed using a Qubit 2.0 fluorometer (Life Technologies) and an Ion Sphere quality control kit (Life Technologies). Ion Torrent chips (316 Chip kit v2; Life Technologies) were prepared and loaded according to the manufacturer's protocol. PGM sequencing (Ion PGM Hi-Q Sequencing Kit; Life Technologies) was done with 500 flows, 18 μs water and argon gas to drive fluidics. Data were analyzed with Torrent Suite 3.0 or higher with alignment against Hg19 and the Variant Caller plugin. The quantitative accuracy was documented using dilutions of *TERT*p-mutant cell line Calu-1 (DSML) in normal DNA (Supplementary Fig. S1). In addition, we determined the diagnostic sensitivity and specificity of our assay by analyzing DNA extracted from the CSF cellular components in patients with non–tumor-related hydrocephalus during shunt implantation ($n = 6$).

Digital PCR

Digital droplet PCR (ddPCR) was performed on a Bio-Rad QX200 using the Bio-Rad TERT C228T_113 Assay (Assay ID dHsaEXD72405942). The detailed method is provided in the Supporting Information.

IDH mutation detection in tumor tissue

IDH1/2 mutation detection was performed in the tumor tissue based on conventional Sanger sequencing, using established primer sets, as published elsewhere by our group (17).

MGMT promoter methylation assessment in tumor tissue

MGMT promoter methylation status was determined by the methylation-specific PCR, as described by Esteller and colleagues (18).

Radiologic evaluation and volumetric measurements

All patients in the study received a pre- and postop. MRI (day one after surgery) with T1, T1 post-contrast, T2, and FLAIR sequences. Radiologic progression was determined using the criteria for Response Assessment in Neuro-Oncology (19). In addition, the preoperative T1-weighted postcontrast MR scans were used to measure the enhancing tumor size and obtain volumetric measurements. A combination of manual segmentation using the ITK-SNAP software (20) and intensity filtering based on individually adjusted thresholds was used to select the enhancing tumor tissue with and without the necrotic tumor portion.

To investigate correlations between the successful detection of *TERT*p-mutant tDNA and tumor location, we used a previously described MRI-based classification of gliomas (21) to assess the spatial relationship of the tumor with the subventricular zone (SVZ) and the cortex as follows:

Group 1	Tumor contacting SVZ and infiltrating cortex
Group 2	Tumor contacting SVZ but not involving cortex
Group 3	Tumor not contacting SVZ but involving cortex
Group 4	Tumor neither contacting SVZ nor infiltrating cortex

Statistical analysis

The Kaplan–Meier technique was used to estimate progression-free survival (PFS) and overall survival (OS) and tested for significance by the log-rank test. PFS was calculated from the day of surgery until MRI-confirmed tumor progression or end of follow-up. OS was defined as the interval from the day of first surgery until death or the end of follow-up. The Mann–Whitney *U* and Fisher exact tests were used to test for association of clinical variables and CSF-tDNA, whereas the Spearman test was used to correlate coefficients among outcomes of the contrast-enhancing tumor volume with the abundance of the mutant CSF-tDNA. Multivariate Cox regression models were applied to assess the impact of CSF-tDNA on patient's outcome. All *P* values are two-sided, and all analyses were conducted using the SPSS software package (Version 21.0 SPSS Inc.).

Results

Patients' characteristics

Out of 60 patients who underwent surgery for an intracranial tumor, we identified 38 patients (24 males and 14 females) with *TERT*p-mutant/*IDH* wild-type glioblastomas who were enrolled into our study (Fig. 1). The median patient age at initial diagnosis was 67.6 years (range, 64.3–71.4 years). Patient characteristics and tumor features are shown in Table 1.

Gross total resection of the enhancing tumor—as evaluated by early postoperative MRI—was achieved in 20 patients, whereas 18 patients underwent a subtotal resection. Radiotherapy was applied in all cases, and 31 patients were treated concomitantly with temozolomide. Temozolomide therapy was prematurely discontinued in 7 patients, due to disease progression, and in 2 patients, because of hematologic toxicities.

Our study had a median follow-up of 12.36 months (4.25–33.0 months). The median PFS of patients with a newly-diagnosed GBM was 5.7 months (4.2–7.2 months), and the median OS was 9.9 months (6.7–13.2 months). Twenty-nine patients (78.3%) died during the time of follow-up. The last update of progression status was performed in April 2018.

*TERT*p mutation detection

The median coverage for tumor tissue samples was 48,170 reads (range, 42,716–60,268 reads); for CSF, it was 48,890 reads (range, 8,680–198,576 reads); and for plasma samples, it was 49,700 reads (range, 6,647–107,900 reads). Using this approach, we could detect *TERT*p mutations in CSF-tDNA at allelic frequencies as low as 0.4% for C228T and 0.2% for C250T. The turnaround time from processing the CSF/plasma sample to final mutation data report was 3 to 5 days.

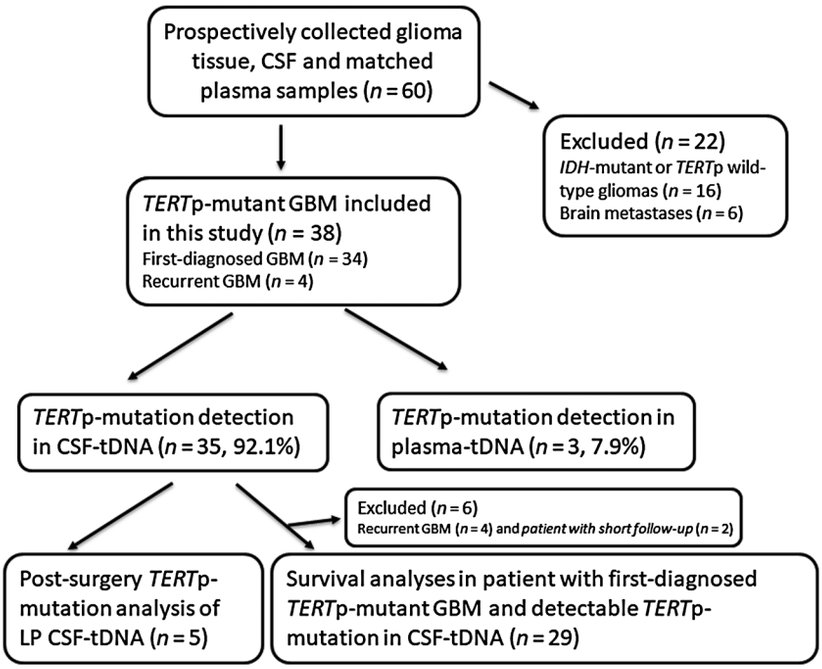

Figure 1.
Schematic representation of the inclusion flow used in this study. GBM, glioblastoma multiforme; LP, lumbar puncture.

In the tumor tissue, the detected *TERT*p hotspot mutations were located at 146 bp (referred to as C250T, $n = 7$) and in 31 cases at 124 bp (referred to as C228T) upstream of the translation start of the *TERT* promoter. In the matched CSF-tDNA, the *TERT*p mutation was successfully detected in 35 of 38 patients (92.1%; Table 1).

Remarkably, in four *IDH*-mutant/*TERT*p-mutant gliomas (oligodendrogliomas), we detected only one *TERT*p mutation in the CSF-tDNA (Supplementary Table S1). In contrast, no *TERT*p mutations were detectable in the CSF-tDNA of any of the patients with an *IDH*-mutant/*TERT*p wild-type glioma ($n = 7$) or an *IDH* wild-type/*TERT*p wild-type glioma ($n = 5$) or in patients with brain metastases ($n = 6$). Additional sequencing of CSF cell-free DNA from 6 patients with a non–tumor-related hydrocephalus revealed no *TERT*p mutations. Taken together, these results show a specificity of 100% (95% CI, 87.6–100%) and a sensitivity of 92.1% (95% CI, 78.6–98.3%) in determining the *TERT*p mutations in the CSF of *TERT*p-mutant glioblastoma patients. Repeated analyses of a subgroup of samples ($n = 15$) from the CSF-tDNA indicated a high reproducibility of our results, with a median SD from mean of 7.6% (range, 1.3%–34.4%).

Moreover, to validate our results, ddPCR was performed in duplicates of five *TERT*p-mutant and four *TERT*p wild-type samples. The ddPCR showed concordant results with those determined by the Ion Torrent system in all 9 cases. However, our study has a limited power to sufficiently address the question which method is superior in terms of *TERT*p mutation detection in the CSF-tDNA.

The sensitivity of *TERT*p mutation assessment in the plasma-tDNA was far lower [7.9% (95% CI, 1.6–21.4%) ($n = 3$)] than that in the CSF (Fisher exact test, $P < 0.0001$). All 3 patients with detectable *TERT*p mutation in plasma-tDNA had large glioblastomas with tumor infiltration of the choroid plexus and encasement of one major cerebral artery.

Association between CSF-ctDNA detection and tumor volume and location

To investigate whether the tumor size might affect the *TERT*p mutation detection in the CSF, we performed volumetric tumor measurements. The median gross tumor volume was 59.2 cm^3 (range, 1.8–177.2 cm^3), and the median contrast-enhancing tumor volume was 45.5 cm^3 (range, 1.5–105.33 cm^3).

Among the 29 newly-diagnosed GBM cases with detectable *TERT*p mutations in the CSF and an available follow-up, we observed a statistically significant linear correlation between the variant allele frequencies (VAF) and either the gross tumor volume (Spearman-Rho = 0.55; $P = 0.002$) or the (Gadolinium-) contrast-enhanced tumor volume (Spearman-Rho = 0.54; $P = 0.003$; Fig. 2).

In terms of anatomical location, all but one tumor was adjacent to the CSF space through infiltration of the subventricular zone and/or the cortical subarachnoidal space (groups 1–3; Fig. 3 and Table 1). Interestingly, the only patient with a tumor that was entirely encapsulated by the brain parenchyma (Group 4, Table 1) was 1 of the 3 patients with nondetectable *TERT*p mutations in the CSF (Supplementary Fig. S2).

Notably, we did not observe a significant association between the *TERT*p mutation VAF in the CSF-tDNA and patients' age, sex, or performance status.

Association between *TERT*p mutation VAF in CSF-tDNA and patients' outcome

To explore a potential role of the *TERT*p mutation VAF in the CSF-tDNA in predicting patients' survival, Kaplan–Meier curves were generated and analyzed based on the *TERT*p mutation VAFs in the CSF-tDNA. It was concordantly observed that patients with low VAF in the CSF-tDNA had a longer OS when compared with patients with high VAF, irrespective of using the

Table 1. Patient characteristics and tumor features

Patient ID	Sex	Age at first surgery (years)	Histology	Extent of resection	*IDH* mutation status/tumor tissue	*MGMT* promoter status
GBM_NCH01	Male	66	GBM	GTR	Wild-type	Unmethylated
GBM_NCH02	Male	75	GBM	STR	Wild-type	Unmethylated
GBM_NCH04	Male	72	GBM	STR	Wild-type	Methylated
GBM_NCH06	Female	72	GBM	STR	Wild-type	Unmethylated
GBM_NCH07	Female	62	GBM	STR	Wild-type	Methylated
GBM_NCH09	Male	64	GBM	GTR	Wild-type	Unmethylated
GBM_NCH10	Male	66	GBM	GTR	Wild-type	Unmethylated
GBM_NCH17	Female	63	GBM	GTR	Wild-type	Unmethylated
GBM_NCH08	Male	62	GBM	STR	Wild-type	Unmethylated
GBM_NCH11	Male	79	GBM	GTR	Wild-type	Unmethylated
GBM_NCH14	Male	57	GBM	STR	Wild-type	Unmethylated
GBM_NCH13	Male	79	GBM	STR	Wild-type	Unmethylated
GBM_NCH19	Female	62	GBM	STR	Wild-type	Methylated
GBM_NCH29	Male	45	GBM	GTR	Wild-type	Unmethylated
GBM_NCH30	Female	67	GBM	GTR	Wild-type	Unmethylated
GBM_NCH33	Male	64	GBM	GTR	Wild-type	Unmethylated
GBM_NCH38	Female	72	GBM	STR	Wild-type	Methylated
GBM_NCH39	Male	76	GBM	GTR	Wild-type	Unmethylated
GBM_NCH41	Female	73	GBM	GTR	Wild-type	Unmethylated
GBM_NCH46	Male	82	GBM	STR	Wild-type	Unmethylated
GBM_NCH49	Male	75	GBM	GTR	Wild-type	Methylated
GBM_NCH50	Female	49	GBM	STR	Wild-type	Methylated
GBM_NCH51	Female	72	GBM	GTR	Wild-type	Unmethylated
GBM_NCH55	Male	61	GBM	STR	Wild-type	Methylated
GBM_NCH58	Female	78	GBM	STR	Wild-type	Unmethylated
GBM_NCH68	Male	53	GBM	GTR	Wild-type	Methylated
GBM_NCH66	Male	77	Recurrent GBM	STR	Wild-type	Methylated
GBM_NCH69	Male	59	GBM	GTR	Wild-type	Methylated
GBM_NCH70	Female	52	Recurrent GBM	GTR	Wild-type	Methylated
GBM_NCH71	Male	71	GBM	GTR	Wild-type	Methylated
GBM_NCH72	Male	67	GBM	STR	Wild-type	Methylated
GBM_NCH74	Female	82	GBM	GTR	Wild-type	Methylated
GBM_NCH75	Male	76	GBM	STR	Wild-type	Unmethylated
GBM_NCH76	Female	72	recurrent GBM	STR	Wild-type	Unmethylated
GBM_NCH56	Male	55	GBM	STR	Wild-type	Unmethylated
GBM_NCH80	Male	83	GBM	GTR	Wild-type	Unmethylated
GBM_NCH83	Male	65	GBM	GTR	Wild-type	Not determined
GBM_NCH53	Female	64	recurrent GBM	GTR	Wild-type	Unmethylated

*TERT*p mutation/ tumor	Intraoperative *TERT*p mutation detection/CSF	Intraoperative VAF/CSF (%)	Postoperative *TERT*p mutation detection/CSF	Postoperative VAF/CSF (%)	*TERT*p mutation detection/plasma
C228T	Yes	20.91	Yes	9.30	No
C250T	No	**0.00**	Not determined		No
C250T	Yes	44.44	Not determined		No
C228T	Yes	60.90	Not determined		No
C250T	Yes	70.03	Not determined		Yes
C228T	Yes	14.80	Not determined		No
C228T	Yes	11.45	Not determined		No
C228T	Yes	4.96	Not determined		No
C228T	Yes	16.41	Not determined		No
C228T	Yes	44.50	Not determined		No
C228T	Yes	12.76	Not determined		No
C228T	Yes	38.54	Not determined		No
C250T	No	**0.13**	Not determined		No
C250T	Yes	2.93	Not determined		No
C228T	Yes	1.76	No	0.18	No
C228T	Yes	3.17	Not determined		No
C228T	Yes	51.95	Not determined		No
C228T	Yes	13.65	Not determined		No
C228T	Yes	20.35	Not determined		Yes
C228T	Yes	33.60	Not determined		No
C228T	Yes	29.56	Not determined		No
C228T	Yes	41.07	Not determined		No
C228T	Yes	20.11	Not determined		Yes

(Continued on the following page)

Table 1. Patient characteristics and tumor features (Cont'd)

*TERT*p mutation/ tumor	Intraoperative *TERT*p mutation detection/CSF	Intraoperative VAF/CSF (%)	Postoperative *TERT*p mutation detection/CSF	Postoperative VAF/CSF (%)	*TERT*p mutation detection/plasma	VAF/plasma (%)	Gross tumor volume (mm^3)	Volume of contrast-enhanced tumor (mm^3)	Tumor location	Outcome
C228T	Yes	20.61	Not determined		No	0.13	66833.53	53724.32	Group 2	Deceased
C228T	Yes	20.93	Not determined		No	0.00	60772.75	32831.29	Group 1	Deceased
C228T	Yes	5.94	No	0.06	No	0.14	74224.45	60968.50	Group 2	Deceased
C228T	Yes	11.01	Not determined		No	0.00	94466.03	61016.54	Group 1	Deceased
C228T	Yes	53.84	No	0.69	No	**10.62**	177251.17	105333.12	Group 1	Deceased
C228T	Yes	11.01	Not determined		No	0.08	81252.39	61840.50	Group 1	Deceased
C228T	Yes	18.82	Not determined		No	0.18	18712.70	14683.15	Group 3	Deceased
C228T	Yes	20.11	Not determined		No	0.12	28823.60	20747.55	Group 3	Deceased
C228T	Yes	38.16	Not determined		No	0.10	Not determined	Not determined	Group 1	Deceased
C228T	No	**0.14**	Not determined		No	0.16	87319.59	62163.09	Group 1	Deceased
C250T	Yes	0.91	Not determined		No	0.21	113304.20	76145.89	Group 1	Deceased
C228T	Yes	3.26	Not determined		No	0.10	27968.99	22998.19	Group 1	Deceased
C250T	Yes	4.47	Not determined		No	0.00	17148.51	12881.53	Group 4	Deceased
C228T	Yes	43.44	Yes	2.92	No	0.17	54706.97	40096.26	Group 1	Deceased
C228T	Yes	19.34	Not determined		No	0.00	44666.13	32815.50	Group 3	Alive
						0.10	72386.63	43229.56	Group 1	Deceased
						0.28	106570.64	101406.47	Group 1	Deceased
						0.08	12296.64	6410.81	Group 3	Deceased
						5.62	50192.29	42088.88	Group 2	Deceased
						0.18	76629.59	48995.72	Group 1	Deceased
						0.13	135806.45	93617.38	Group 2	Deceased
						0.23	75922.40	56703.61	Group 2	Deceased
						35.38	20767.32	15543.69	Group 2	Deceased
						0.13	88345.95	54917.92	Group 3	Deceased
						0.15	85023	59706.00	Group 1	Deceased
						0.12	3616.69	3033.74	Group 3	Alive
						0.45	10459.59	9188.76	Group 1	Deceased
						0.15	66185.46	47871.99	Group 1	Alive
						0.11	79877.23	48156.71	Group 1	Alive
						0.12	38323.30	17340.88	Group 2	Deceased
						0.22	57268.27	24060.59	Group 3	Alive
						0.17	56731.03	14887.91	Group 1	Alive
						0.11	62396.41	60236.68	Group 1	Deceased
						0.15	38811.85	16240.43	Group 1	Deceased
						0.17	39343.98	24915.7	Group 2	Deceased
						0.025	Not determined	Not determined	Group 1	alive -short follow-up
						0.03	Not determined	Not determined	Group 3	alive -short follow-up
						0.13	1875.9	1503.4	Group 2	lost from follow-up

Abbreviations: GBM, glioblastoma multiforme; GTR, gross total resection; STR, sub-total resection.

lower quartile VAF of 11.45%, the lower third VAF of 13%, or the median VAF of 20.3% to dichotomize the patients ($P = 0.035$, $P = 0.008$, and $P = 0.062$, respectively; Fig. 4).

To substantiate our findings, a multivariate analysis was performed including all first-diagnosed glioblastoma patients with detectable *TERT*p-mutant CSF-tDNA and available follow-up ($n = 29$). The *TERT*p mutation VAF with a cutoff of 13% was found to be an independent prognostic factor for OS [$P = 0.001$, HR = 16.02; 95% confidence interval (CI), 3.15–28.43; Table 2]. By exploring an interaction between the tumor volume and a *TERT*p mutation VAF cutoff of 13% in the CSF-tDNA as one factor in the multivariate analysis, the HR was 2.07 (95% CI, 1.33–3.22, $P = 0.001$). All other included clinical parameters such as age, extent of resection,

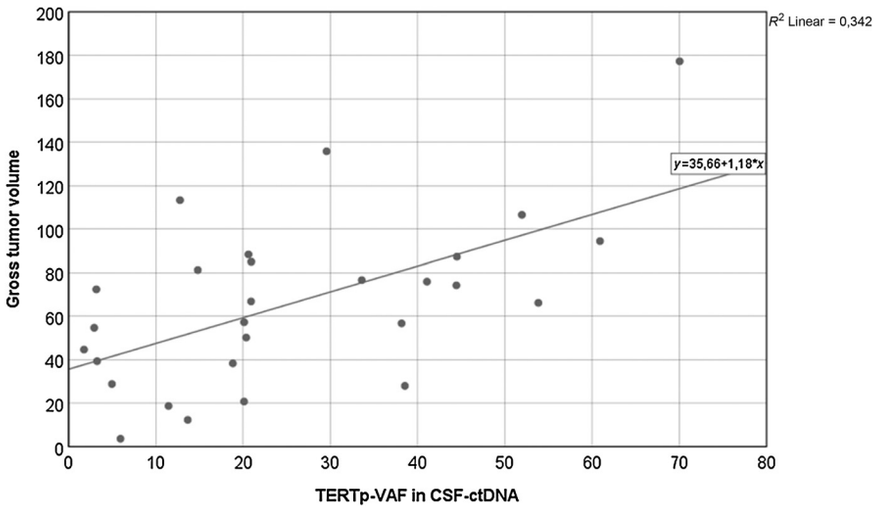

Figure 2.
Linear regression between the VAFs and tumor volume among the 29 cases in which detectable TERTp mutation was found in the CSF-ctDNA. Statistically significant linear correlations between the VAFs and either the gross tumor volume (Spearman-Rho = 0.55; $P = 0.002$) and the (Gadolinium-) contrast-enhanced tumor volume (Spearman-Rho = 0.54; $P = 0.003$) were observed.

and *MGMT* promoter status were not independent prognostic factors in our cohort, although it is possible that there are other clinical variables which may account for the differences in outcome.

Postoperative *TERT*p mutation detection in the CSF-tDNA

To examine a potential application of CSF-tDNA as a marker for postoperative residual disease, CSF was collected in 5 patients who had intraoperatively detectable *TERT*p mutation in the CSF-tDNA and underwent a lumbar drainage placement to treat a postoperative CSF leakage. Interestingly, we saw a dramatic decrease of VAF levels ($P = 0.043$, Wilcoxon-signed rank test; Supplementary Fig. S3). However, although GTR was achieved in all 5 patients, *TERT*p mutation in the CSF-tDNA was postoperatively detectable in only two cases. Remarkably, persistent postoperative *TERT*p mutation detection in the lumbar spine CSF was associated with a decreased PFS of both patients (5.1 months), compared with the 3 patients with nondetectable mutation who had a longer PFS (median, 11.9 months; 95% CI, 8.3–15.5 months). However, given the small group of patients, our study was likely underpowered to make any significant conclusions about differences in survival outcomes.

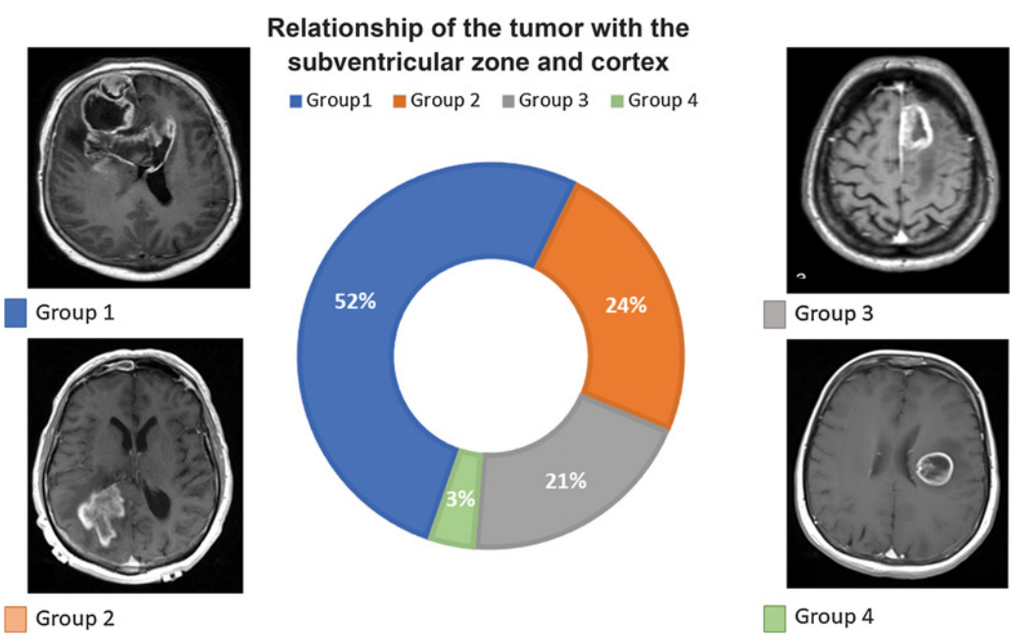

Figure 3.
The MRI-based classification of the tumor location in 38 patients with *IDH* wild-type/ *TERT*p-mutant glioblastomas to assess the spatial relationship with the ventricle system and cortex with an example of every group subventricular zone (SVZ). Group 1: Tumor contacting SVZ and infiltrating cortex (52%); Group 2: Tumor contacting SVZ but not involving cortex (24%); Group 3: Tumor not contacting SVZ but involving cortex (21%); Group 4: Tumor neither contacting SVZ nor infiltrating cortex (3%).

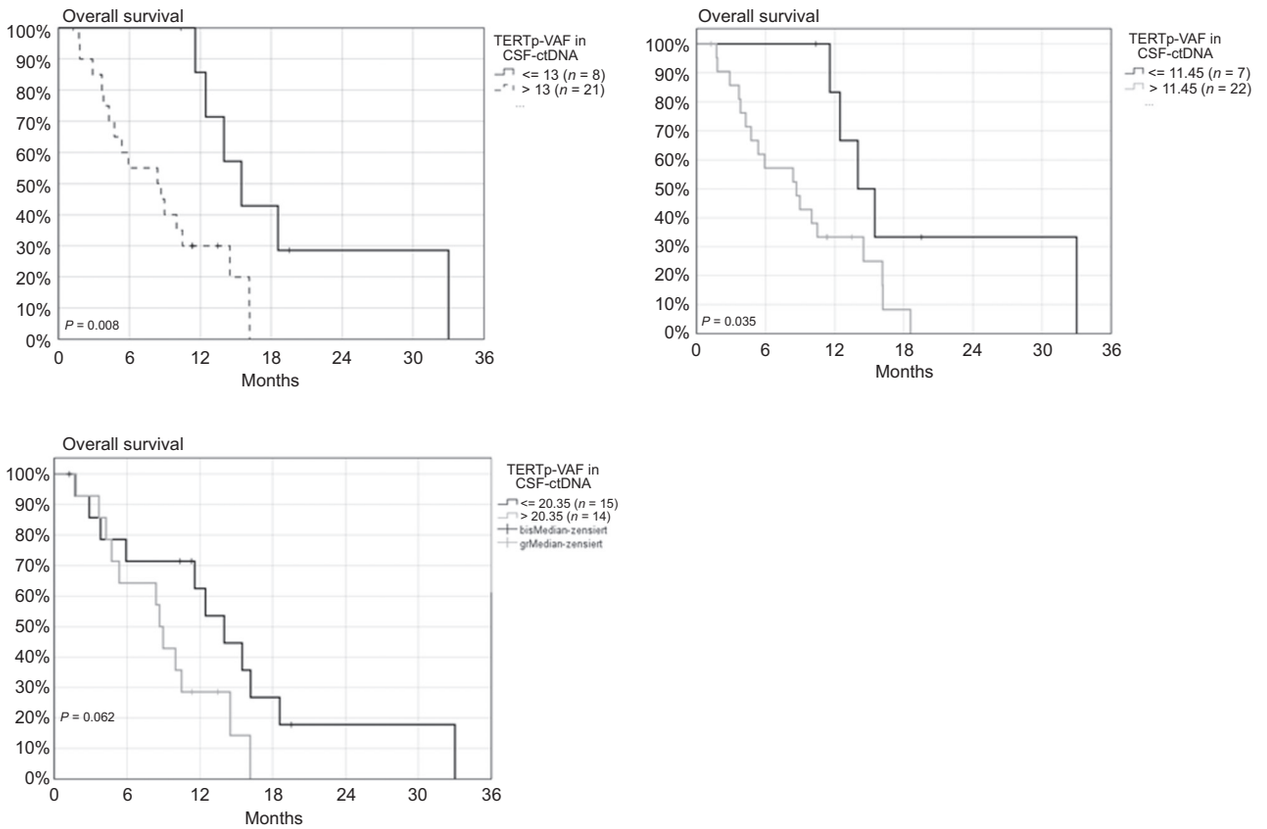

Figure 4.

Kaplan–Meier estimates of OS. The detected *TERT*p mutation tDNA-VAF shows a significant prognostic value on patients' survival. Patients with low VAF in the CSF-tDNA have longer OS when compared with patients with high VAF, irrespective of using the lower quartile VAF [11.45%; 14.0 mo. (95% CI, 10.3–17.6) vs. 8.6 mo. (95% CI, 4.1–13.2), $P = 0.035$], the lower third VAF [13%; 15.4 mo. (95% CI, 11.6–19.2) vs. 8.3 mo. (95% CI, 2.3–14.4), $P = 0.008$], or the median VAF [20.3%; 14.0 mo. (95% CI, 9.2–18.7) vs. 8.6 mo. (95% CI, 7.5–9.8), $P = 0.062$] to dichotomize the patients.

Discussion

Detection of circulating tumor material has been shown to be of clinical value for diagnosis, prediction of response to treatment, and prognosis in cancer patients (10, 11, 14, 15, 22). In this pilot study, we demonstrate that *TERT*p mutation detection in intraoperatively collected CSF is feasible with a very high sensitivity and specificity in glioblastoma with spatial relationship to a CSF reservoir in the brain, consistent with the findings from previous studies (23, 24). Remarkably, we observed a significant association between the VAF of the *TERT*p mutation in the CSF-tDNA and the outcome of glioblastoma patients in our cohort. Using different cutoffs, our data consistently showed that an increasing burden of *TERTp*-mutant alleles in the CSF-tDNA was associated with unfavorable outcomes, suggesting a high reliability of the *TERT*p mutation VAF levels in the CSF-tDNA as an outcome prediction tool in glioblastoma patients.

Furthermore, we found a lower sensitivity of *TERT*p mutation detection in a distinct subset of *TERT*p-mutant/*IDH*-mutant gliomas (oligodendrogliomas), confirming the findings of a recent study that reported on the inability to detect molecular alterations in the CSF-tDNA in some low-grade gliomas (24). This may be explained by the higher cellularity of glioblastomas compared with oligodendrogliomas, which is presumably associated with larger quantities of tDNA shedding into the CSF.

A further potential application for CSF-tDNA is its use as a marker for postoperative residual disease. Presently, predicting the disease-free status of patients is predominantly based on clinical and radiologic criteria. Interestingly, fluctuations in circulating tDNA levels have been shown to occur prior

Table 2. Stepwise Backward Logistic Regression for overall survival performed in glioblastoma patients with detectable *TERT*p-mutant CSF-tDNA and available follow-up ($n = 29$)

	HR (95% CI)	*P* value
Age $\geq$ 65 years	0.49 (0.18–1.32)	0.16
Gross tumor volume	1.44 (0.55–3.77)	0.45
Contrast-enhanced tumor volume	0.51 (0.11–2.26)	0.37
Complete resection of contrast-enhanced tumor	1.03 (0.37–2.88)	0.94
MGMT promoter methylation status	0.31 (0.12–1.01)	0.87
VAF of *TERT*p mutation in the CSF-tDNA (cutoff 13%)	16.02 (3.15–28.43)	0.001

NOTE: The *TERT*p-mutation VAF was found to be an independent prognostic factor for OS ($P = 0.001$, HR = 16.02, 95% CI: 3.15–28.43).

to changes seen in imaging studies (10). Moreover, it has been demonstrated that levels of circulating tDNA increase with disease progression and correspondingly decrease with response to therapy in solid tumors and glioblastomas (10, 11, 25, 26). In the current study, we demonstrate an association between patients' outcome and intra-/postoperative *TERT*p mutation CSF-tDNA levels in five cases. A significant postoperative reduction of the *TERT*p mutation VAF in the CSF-DNA when compared with the "baseline" intraoperative VAF level was associated with favorable survival outcomes. Although preliminary, this finding suggests that clearance of *TERT*p mutations in the CSF may indicate residual disease in glioblastoma patients and may be used for disease monitoring. However, this observation needs to be verified in a larger cohort of patients before any definitive conclusions can be made.

In concordance with earlier studies, our assay to detect *TERT*p-mutant plasma-tDNA had a low sensitivity (12). Diaz and colleagues reported that mutant DNA fragments were found in high concentrations in the circulation of most patients with metastatic cancer—e.g., melanoma, breast, or colon cancers—and at lower concentrations in patients with localized cancers, as in gliomas or prostate cancer (13, 27). Similarly, a recent study showed that levels of CSF-tDNA were considered significantly enriched when compared with the corresponding plasma in 12 individuals with primary or metastatic brain tumors (28). In order to improve this shortcoming, new technologies are needed. For instance, an innovative technique employed focused ultrasound to increase the release of brain tumor material into the bloodstream, essentially making blood a viable surrogate for tumor detection (29).

Although we suggest that *TERT*p mutation detection in the CSF-tDNA has the potential to be developed as a diagnostic instrument in the management of glioblastoma patients, we acknowledge that our approach to collect CSF at the time of surgery was not intended as a preoperative diagnostic tool. From a clinical standpoint, the preoperative detection of *TERT*p mutation in the CSF-tDNA by lumbar puncture would be more readily accessible than by intraoperative surgery, notwithstanding the consideration of lumbar punctures as an invasive procedure. Consequently, the assessment of genomic alterations at several longitudinal time points as a "liquid biopsy" is a consequential approach to monitor tumor progression and to correlate with radiographic findings. Ultimately, this serial approach may avoid unnecessary surgical procedures and lead to better management of glioblastoma patients. Lastly, a recent study showed a very low congruence for same patient-paired prostate cancer samples between different laboratories (30), raising the question whether the results generated by our assay could be generalized to other laboratories or attained by using different assays. Therefore, to complement our study, confirmatory observational cohorts with more patients and further techniques are certainly needed to determine precise cutoffs of the *TERT*p mutation VAF that may be used to define patients at high risk for rapid progression.

In conclusion, our pilot study highlights the value of CSF-tDNA for an accurate and reliable detection of *TERT*p mutations in glioblastomas. Furthermore, our findings suggest that high *TERT*p mutation VAF levels in the CSF-tDNA may be a suitable predictor of poor survival in glioblastoma patients. This would allow for a more precise risk stratification of patients for clinical trials. Further studies are needed to validate the findings of this exploratory analysis.

Disclosure of Potential Conflicts of Interest

C. Thiede is an employee of AgenDx GmbH, reports receiving speakers bureau honoraria from Illumina, Novartis, and Roche, is a consultant/advisory board member for Novartis and Roche, and reports receiving commercial research grants from Bayer and Novartis. No potential conflicts of interest were disclosed by the other authors.

Disclaimer

The content is solely the responsibility of the authors and does not necessarily represent the official views of Harvard Catalyst, Harvard University and its affiliated academic healthcare centers, or the NIH.

Authors' Contributions

Conception and design: T.A. Juratli, D. Krex, C. Thiede
Development of methodology: T.A. Juratli, A. Zolal, C. Schuster, D. Krex, C. Thiede
Acquisition of data (provided animals, acquired and managed patients, provided facilities, etc.): T.A. Juratli, S. Stasik, S. Richter, D. Daubner, S. Hennig, M. Makina, T. Lautenschlaeger, G. Schackert, D. Krex, C. Thiede
Analysis and interpretation of data (e.g., statistical analysis, biostatistics, computational analysis): T.A. Juratli, S. Stasik, A. Zolal, D. Daubner, M.A. Juratli, S. Hennig, M. Meinhardt, T. Lautenschlaeger, D. Krex
Writing, review, and/or revision of the manuscript: T.A. Juratli, A. Zolal, M.A. Juratli, S. Hennig, M. Meinhardt, T. Lautenschlaeger, G. Schackert, D. Krex, C. Thiede
Administrative, technical, or material support (i.e., reporting or organizing data, constructing databases): T.A. Juratli, D. Daubner, R. Thowe, D. Krex
Study supervision: T.A. Juratli, D. Krex

Acknowledgments

The authors thank Drs. Dino Podlesek, Stephan Sobottka, Matthias Kirsch, and Thomas Pinzer for helping collect CSF.

This work was conducted with support from Harvard Catalyst|The Harvard Clinical and Translational Science Center (National Center for Research Resources and the National Center for Advancing Translational Sciences, NIH Award UL1 TR001102) and financial contributions from Harvard University and its affiliated academic healthcare centers.

This work is supported by the MeDDrive (grant number 60.378) to Dr. T.A. Juratli and the BMBF (grant 01GS0872) to Dr. C. Thiede. Dr. T.A. Juratli was awarded the Aesculap EANS research Prize 2018 for this study.

The costs of publication of this article were defrayed in part by the payment of page charges. This article must therefore be hereby marked *advertisement* in accordance with 18 U.S.C. Section 1734 solely to indicate this fact.

Received December 14, 2017; revised May 4, 2018; accepted June 19, 2018; published first June 25, 2018.

References

1. Parsons DW, Jones S, Zhang X, Lin JC, Leary RJ, Angenendt P, et al. An integrated genomic analysis of human glioblastoma multiforme. Science 2008;321:1807–12.
2. Brat DJ, Verhaak RG, Aldape KD, Yung WK, Salama SR, Cooper LA, et al. Comprehensive, integrative genomic analysis of diffuse lower-grade gliomas. N Engl J Med 2015;372:2481–98.

3. Verhaak RG, Hoadley KA, Purdom E, Wang V, Qi Y, Wilkerson MD, et al. Integrated genomic analysis identifies clinically relevant subtypes of glioblastoma characterized by abnormalities in PDGFRA, IDH1, EGFR, and NF1. Cancer Cell 2010;17:98–110.
4. Wakimoto H, Tanaka S, Curry WT, Loebel F, Zhao D, Tateishi K, et al. Targetable signaling pathway mutations are associated with malignant phenotype in IDH-mutant gliomas. Clin Cancer Res 2014;20: 2898–909.
5. Lai A, Kharbanda S, Pope WB, Tran A, Solis OE, Peale F, et al. Evidence for sequenced molecular evolution of IDH1 mutant glioblastoma from a distinct cell of origin. J Clin Oncol 2011;29:4482–90.
6. Brastianos PK, Nayyar N, Rosebrock D, Leshchiner I, Gill CM, Livitz D, et al. Resolving the phylogenetic origin of glioblastoma via multifocal genomic analysis of pre-treatment and treatment-resistant autopsy specimens. npj Precision Oncology 2017;1:33.
7. Simon M, Hosen I, Gousias K, Rachakonda S, Heidenreich B, Gessi M, et al. TERT promoter mutations: a novel independent prognostic factor in primary glioblastomas. Neuro Oncol 2015;17:45–52.
8. Eckel-Passow JE, Lachance DH, Molinaro AM, Walsh KM, Decker PA, Sicotte H, et al. Glioma groups based on 1p/19q, IDH, and TERT promoter mutations in tumors. N Engl J Med 2015;372:2499–508.
9. Maheswaran S, Sequist LV, Nagrath S, Ulkus L, Brannigan B, Collura CV, et al. Detection of mutations in EGFR in circulating lung-cancer cells. N Engl J Med 2008;359:366–77.
10. Dawson SJ, Rosenfeld N, Caldas C. Circulating tumor DNA to monitor metastatic breast cancer. N Engl J Med 2013;369:93–4.
11. Murtaza M, Dawson SJ, Tsui DW, Gale D, Forshew T, Piskorz AM, et al. Non-invasive analysis of acquired resistance to cancer therapy by sequencing of plasma DNA. Nature 2013;497:108–12.
12. Bettegowda C, Sausen M, Leary RJ, Kinde I, Wang Y, Agrawal N, et al. Detection of circulating tumor DNA in early- and late-stage human malignancies. Sci Transl Med 2014;6:224ra24.
13. Diaz LA, Bardelli A. Liquid biopsies: genotyping circulating tumor DNA. J Clin Oncol 2014;32:579–86.
14. Figg WD, Reid J. Monitor tumor burden with circulating tumor DNA. Cancer Biol Ther 2013;14:697–8.
15. Germano G, Mauri G, Siravegna G, Dive C, Pierce J, Di Nicolantonio F, et al. Parallel evaluation of circulating tumor DNA and circulating tumor cells in metastatic colorectal cancer. Clin Colorectal Cancer 2018;17:80–3.
16. Stasik S, Schuster C, Ortlepp C, Platzbecker U, Bornhäuser M, Schetelig J, et al. An optimized targeted next-generation sequencing approach for sensitive detection of single nucleotide variants. Biomol Detect Quantif 2018;15:6–12.
17. Juratli TA, Kirsch M, Robel K, Soucek S, Geiger K, von Kummer R, et al. IDH mutations as an early and consistent marker in low-grade astrocytomas WHO grade II and their consecutive secondary high-grade gliomas. J Neurooncol 2012;108:403–10.
18. Esteller M, Garcia-Foncillas J, Andion E, Goodman SN, Hidalgo OF, Vanaclocha V, et al. Inactivation of the DNA-repair gene MGMT and the clinical response of gliomas to alkylating agents. N Engl J Med 2000;343: 1350–4.
19. Wen PY, Macdonald DR, Reardon DA, Cloughesy TF, Sorensen AG, Galanis E, et al. Updated response assessment criteria for high-grade gliomas: response assessment in neuro-oncology working group. J Clin Oncol 2010;28:1963–72.
20. Yushkevich PA, Piven J, Hazlett HC, Smith RG, Ho S, Gee JC, et al. User-guided 3D active contour segmentation of anatomical structures: significantly improved efficiency and reliability. Neuroimage 2006;31:1116–28.
21. Lim DA, Cha S, Mayo MC, Chen MH, Keles E, VandenBerg S, et al. Relationship of glioblastoma multiforme to neural stem cell regions predicts invasive and multifocal tumor phenotype. Neuro Oncol 2007; 9:424–9.
22. Juratli MA, Sarimollaoglu M, Nedosekin DA, Melerzanov AV, Zharov VP, Galanzha EI. Dynamic fluctuation of circulating tumor cells during cancer progression. Cancers (Basel) 2014;6:128–42.
23. Wang Y, Springer S, Zhang M, McMahon KW, Kinde I, Dobbyn L, et al. Detection of tumor-derived DNA in cerebrospinal fluid of patients with primary tumors of the brain and spinal cord. Proc Natl Acad Sci U S A 2015;112:9704–9.
24. Martínez-Ricarte F, Mayor R, Martínez-Sáez E, Rubio-Pérez C, Pineda E, Cordero E, et al. Molecular diagnosis of diffuse gliomas through sequencing of cell-free circulating tumour DNA from cerebrospinal fluid. Clin Cancer Res 2018;24:2812–9.
25. Ahronian LG, Corcoran RB. Strategies for monitoring and combating resistance to combination kinase inhibitors for cancer therapy. Genome Med 2017;9:37.
26. Shao H, Chung J, Lee K, Balaj L, Min C, Carter BS, et al. Chip-based analysis of exosomal mRNA mediating drug resistance in glioblastoma. Nat Commun 2015;6:6999.
27. Diaz LA, Williams RT, Wu J, Kinde I, Hecht JR, Berlin J, et al. The molecular evolution of acquired resistance to targeted EGFR blockade in colorectal cancers. Nature 2012;486:537–40.
28. De Mattos-Arruda L, Bidard FC, Won HH, Cortes J, Ng CK, Peg V, et al. Establishing the origin of metastatic deposits in the setting of multiple primary malignancies: the role of massively parallel sequencing. Mol Oncol 2014;8:150–8.
29. Zhu L, Cheng G, Ye D, Nazeri A, Yue Y, Liu W, et al. Focused ultrasound-enabled brain tumor liquid biopsy. Sci Rep 2018;8:6553.
30. Torga G, Pienta KJ. Patient-paired sample congruence between 2 commercial liquid biopsy tests. JAMA Oncol 2018;4:868–70.